Tryptic Digestion of Soybean Lipoxygenase-1 Generates a 60 kDa Fragment with Improved Activity and Membrane Binding Ability[†]

Mauro Maccarrone,*,[‡] Maria Luisa Salucci,[§] Guus van Zadelhoff,[||] Francesco Malatesta,[§] Gerrit Veldink,[||] Johannes F. G. Vliegenthart,[||] and Alessandro Finazzi-Agrò*,[‡]

Department of Experimental Medicine and Biochemical Sciences, University of Rome, "Tor Vergata", Rome, Italy, Department of Pure and Applied Biology, University of L'Aquila, L'Aquila, Italy, and Bijvoet Center for Biomolecular Research, Department of Bio-organic Chemistry, Utrecht University, Utrecht, The Netherlands

ABSTRACT: Lipoxygenases are key enzymes in the metabolism of unsaturated fatty acids. Soybean lipoxygenase-1 (LOX-1), a paradigm for lipoxygenases isolated from different sources, is composed of two domains: a ~30 kDa N-terminal domain and a ~60 kDa C-terminal domain. We used limited proteolysis and gel-filtration chromatography to generate and isolate a ~60 kDa fragment of LOX-1 ("mini-LOX"), produced by trypsin cleavage between lysine 277 and serine 278. Mini-LOX was subjected to N-terminal sequencing and to electrophoretic, chromatographic, and spectroscopic analysis. Mini-LOX was found to be more acidic and more hydrophobic than LOX-1, and with a higher content of α-helix. Kinetic analysis showed that mini-LOX dioxygenates linoleic acid with a catalytic efficiency approximately 3-fold higher than that of LOX-1 (33.3×10^6 and 10.9×10^6 $M^{-1} \cdot s^{-1}$, respectively), the activation energy of the reaction being 4.5 ± 0.5 and 8.3 ± 0.9 $kJ \cdot mol^{-1}$ for mini-LOX and LOX-1, respectively. Substrate preference, tested with linoleic, α-linolenic, and arachidonic acids, and with linoleate methyl ester, was the same for LOX-1 and mini-LOX, and also identical was the regio- and stereospecificity of the products generated thereof, analyzed by reversed-phase and chiral high-performance liquid chromatography, and by gas chromatography/mass spectrometry. Mini-LOX was able to bind artificial vesicles with higher affinity than LOX-1, but the binding was less affected by calcium ions than was that of LOX-1. Taken together, these results suggest that the N-terminal domain of soybean lipoxygenase-1 might be a built-in inihibitor of catalytic activity and membrane binding ability of the enzyme, with a possible role in physio-(patho)logical conditions.

Lipoxygenases are a family of monomeric non-heme, non-sulfur iron dioxygenases which catalyze the conversion of unsaturated fatty acids into conjugated hydroperoxides. Mammalian lipoxygenases have been implicated in the pathogenesis of several inflammatory conditions such as arthritis, psoriasis, and bronchial asthma (*1*). They have been also implicated in atherosclerosis (*2*), brain aging (*3*), HIV infection (*4*), and kidney disease (*5, 6*). In plants, lipoxygenases favor germination and participate in the synthesis of traumatin and jasmonic acid and in the response to abiotic stress (*7*). Recently, they have been also shown to initiate the programmed death (apoptosis) of plant cells (*8*). Soybean lipoxygenase-1 (LOX-1)[1] is widely used as a prototype for studying the homologous family of lipoxygenases from tissues of different species, both in structural (*9*−*13*) and in

kinetic (*14*−*18*) investigations. The amino acid sequence (*19*) and three-dimensional structure (*9, 10*) of LOX-1 have been determined. The overall 839 amino acid residues of LOX-1, with a molecular mass of 93 840 Da, show 2 domains. The first 146 N-terminal amino acid residues form an 8-stranded β-barrel, and the remaining 693 residues of the C-terminal domain are organized into 23 helices and 8 β-strands. Mammalian lipoxygenases do not have the N-terminal domain present in LOX-1 and other related plant lipoxygenases, thus showing smaller molecular mass (75−80 kDa compared to 94−104 kDa in plants). It has been suggested that the N-terminal domain in LOX-1 makes only a loose contact with the C-terminal domain (*9*), and that it may be also dispensable for plant lipoxygenases (*10*), because all the amino acid side chains responsible for catalysis are

---

* To whom correspondence should be addressed. Telephone and fax: 39-06-72596468. E-mail: Finazzi@uniroma2.it, maccarrone@med.uniroma2.it.

[‡] University of Rome.
[§] University of L'Aquila.
[||] Utrecht University.

[1] Abbreviations: CD, circular dichroism; DDQ, 2,3-dichloro-5,6-dicyano-1,4-benzoquinone; ELISA, enzyme-linked immunosorbent assay; ETE, arachidonic acid; GC/MS, gas chromatography/mass spectroscopy; 13-H(P)OD (-Me), 13-hydro(pero)xy-9,11-(*E,Z*)-octa-decadienoic acid (methyl ester); 13-H(P)OT (-Me), 13-hydro(pero)xy-9,11,15-(*Z,E,Z*)-octadecatrienoic acid (methyl ester); 15-H(P)ETE (-Me), 15-hydro(pero)xy-5,8,11,13-(*Z,Z,Z,E*)-eicosatetraenoic acid (methyl ester); IEF, isoelectric focusing; LOX-1, lipoxygenase-1; OA, oleic acid; OD, linoleic acid; OT, α-linolenic acid; RP-HPLC, reversed-phase high-performance liquid chromatography; SPE, solid-phase extraction.

located in the C-terminal domain. However, limited proteolysis experiments indicated that the two domains are instead tightly associated (*20*), and that domain−domain interactions play a role in the reversible unfolding of LOX-1 (*21, 22*), through ionic interactions (*13*). Despite these structural data, there is no clear evidence whether the N-terminal domain may affect lipoxygenase activity, with respect to the kinetic properties of the reaction and to the product specificity. This seems an important issue, because there is no consensus on how substrates gain access to the metal center and how the N-terminal β-barrel domain may contribute to substrate binding (reviewed in ref *22*).

In this paper, we provide evidence that the removal of the N-terminal domain of LOX-1 by trypsin digestion generates a ∼60 kDa fragment which dioxygenates linoleic acid with enhanced catalytic efficiency. We also show that the shortened form of the enzyme (referred to as "mini-LOX") binds to negatively charged, unsaturated liposomes more efficiently than does LOX-1, while calcium ions are less effective in enhancing the binding. Altogether, these results suggest that the N-terminal domain does affect LOX-1 activity, possibly by regulating substrate binding. They also indicate that the N-terminal domain contains a potential calcium binding site, which might be involved in tuning the interaction of LOX-1 with biological membranes.

EXPERIMENTAL PROCEDURES

Materials. All chemicals were of the purest analytical grade. Linoleic (9,12-octadecadienoic, OD), α-linolenic (9,-12,15-octadecatrienoic, OT), and arachidonic (5,8,11,14-eicosatetraenoic, ETE) acids, pyridine, 1,1,1,3,3,3-hexamethyldisilazane, and chlorotrimethylsilane were from Fluka (Buchs, Switzerland). Sodium borohydride, 3,5-dimethoxy-4-hydroxycinnamic acid, oleic (9-octadecenoic, OA) acid, *N*-tosyl-L-phenylalanine chloromethyl ketone (TPCK)-treated trypsin, and soybean trypsin inhibitor were from Sigma Chemical Co. (St. Louis, MO). Palladium on calcium carbonate (5% Pd) and 2,3-dichloro-5,6-dicyano-1,4-benzoquinone (DDQ) were from Acros Organics (Zwijndrecht, The Netherlands). Tetrahydrofuran and methanol were from Biosolve (Valkenswaard, The Netherlands).

Trypsin Digestion and Activity Assay. Lipoxygenase-1 (linoleate:oxygen oxidoreductase, EC 1.13.11.12; LOX-1) was purified from soybean [*Glycine max* (L.) Merrill, Williams] seeds as reported (*23*). Protein concentration was determined according to Bradford (*24*), using bovine serum albumin as a standard. Trypsin digestions were carried out by treating 200 μL aliquots of LOX-1 (7 mg/mL in 0.2 M Tris·HCl, pH 8.0) with 20 μL aliquots of TPCK-treated trypsin (7 mg/mL in 0.2 M Tris·HCl, pH 8.0) for 30 min at 25 °C. Reactions were stopped by addition of 60 μL aliquots of soybean trypsin inhibitor (7 mg/mL in 0.2 M Tris·HCl, pH 8.0) (*20*). Dioxygenase activity of LOX-1 and mini-LOX in 100 mM sodium borate buffer (pH 9.0) was assayed spectrophotometrically at 25 °C by recording the formation of conjugated hydroperoxides from the different substrates (linoleic, linolenic, or arachidonic acid, or linoleate methyl ester), at 234 nm (*14*). Thermal stability and pH dependence of LOX-1 and mini-LOX were studied as reported (*25*). Activation energy values were calculated according to Segel

(*26*). Kinetic and inhibition studies were performed using different substrate concentrations (in the 0−120 μM range) and three different concentrations (20, 40, or 80 μM) of inhibitor to calculate the kinetic parameters. The experimental points were analyzed by nonlinear regression through the Prism 3 program (GraphPad Software for Science, San Diego, CA).

Electrophoretic, Chromatographic, and Spectroscopic Analysis. Electrophoretic analysis of native LOX-1 and its trypsin-digested fragments (20 μg of protein/lane) was performed under reducing conditions on 12% SDS−polyacrylamide gels, using a Mini-Protean II apparatus (Bio-Rad, Richmond, CA) with 0.75 mm spacer arms (*25*). The prestained molecular mass markers myosin (204 kDa), β-galactosidase (120 kDa), bovine serum albumin (80 kDa), ovalbumin (50 kDa), carbonic anhydrase (34 kDa), soybean trypsin inhibitor (29 kDa), and lysozyme (22 kDa) were from Bio-Rad. Native isoelectric focusing (IEF) was performed in the Mini Protean II apparatus, using a 5% polyacrylamide gel containing ampholytes in the pH range 5.0−9.0 (Sigma), as described (*27*). IEF was calibrated by running the following isoelectric point (p*I*) markers (Sigma): lentil (*Lens culinaris*) lectin (8.8, 8.6, and 8.2), myoglobin from horse heart (7.2 and 6.8), carbonic anhydrase I from human erythrocytes (6.6), and carbonic anhydrase II from bovine erythrocytes (5.9). Gels were stained with Coomassie Brilliant Blue stain.

Chromatographic separation of the fragments of trypsin-digested LOX-1was performed by high-performance liquid chromatography (HPLC) gel filtration on a Biosep-SEC-S3000 column (600 × 7.8 mm, Phenomenex, Torrance, CA). The column was calibrated using standard proteins of known molecular mass (phosphorylase *b*, 97 kDa; bovine serum albumin, 68 kDa; ovalbumin, 44 kDa; carbonic anhydrase, 30 kDa; lysozyme, 14.4 kDa; all from Sigma) with a Perkin-Elmer 1022 LC Plus liquid chromatograph (Norwalk, CO). Samples (50 μg of proteins/injection) were run at a flow rate of 1.0 mL/min, using 0.3 M NaCl in 0.1 M sodium phosphate (pH 7.0) as mobile phase, and chromatograms were recorded at 280 nm. Fractions corresponding to the ∼60 kDa peak were pooled, dialyzed against water for 24 h at 4 °C, and concentrated to 2 mg of proteins/mL using a Centricon 30 ultrafiltration unit (Amicon, Beverly, MA) with a 30 kDa cutoff membrane (*21*). The purified ∼60 kDa fragment of LOX-1, referred to as "mini-LOX", was used in all subsequent analyses. In some experiments, the LOX-1 tryptic fragments of molecular mass <60 kDa were pooled together and concentrated with a Centricon 10 ultrafiltration unit (10 kDa cutoff), and were added to mini-LOX in order to "reconstitute" LOX-1. In another set of experiments, trypsin-digested LOX-1 (100 μg of proteins) was subjected to reversed-phase (RP)-HPLC on a Vydac 208 TP54 column (C8, 250 × 4.6 mm, Phenomenex). In this case, separations were performed at a flow rate of 1.0 mL/min, using 0.2% trifluoroacetic acid as eluent A and 0.2% trifluoroacetic acid, 75% acetonitrile, and 25% 2-propanol as eluent B. A linear gradient from 0% to 100% B was developed in 30 min, recording the chromatograms at 220 nm. In RP-HPLC runs, trypsin-digested LOX-1 eluted as a main peak at 27 min, which was collected and used for sequencing the N-terminal amino acids (as detailed below). The same RP-HPLC analysis of native LOX-1 showed a main peak eluting at 24

min, which was not detectable in the trypsin-digested LOX-1 samples.

For spectroscopic analysis of lipoxygenase, all spectra were recorded in 100 mM Tris·HCl, pH 7.0, at 20 °C (*12*), maintaining the cell temperature by circulating water through a thermojacketed holder. LOX-1 and mini-LOX were used at 10 μM, for recording UV spectra, or at 250 nM, for recording fluorescence and circular dichroism spectra. UV absorption spectra were recorded with a diode-array Hewlett-Packard 8453 spectrophotometer (Hewlett-Packard, Amstelveen, The Netherlands). Fluorescence emission spectra were recorded with a Spex Fluoromax fluorometer (Fluoromax Instruments S. A., Paris, France). The excitation wavelength was 284 nm, and emission spectra were recorded between 300 and 400 nm in 1 cm path length cuvettes. Circular dichroism (CD) spectra (16-fold averaged) were recorded in 1 cm path length cuvettes with a Jasco 5-710 spectropolarimeter (Jasco, Maarssen, The Netherlands), equipped with a 150 W xenon lamp. Prior to spectral acquisition, the spectropolarimeter was fluxed with dry N_2 for at least 30 min. $\Delta\epsilon$ values ($M^{-1}\cdot cm^{-1}$) were calculated from the observed instrument output (ϕ, in millidegrees), the protein concentration (c, in molar), and the number of peptide bonds (n), according to the formula: $\Delta\epsilon = \phi/3300cn$ (*28*).

Sequence Determination and Molecular Graphics. The N-terminal amino acid sequence of mini-LOX was determined by automated Edman degradation using a Perkin-Elmer model AB476A sequencer. Samples (0.2−0.5 nmol) were loaded onto a poly(vinylidene difluoride) membrane (Problott, Perkin-Elmer) coated with Polybrene, as reported (*29*). Molecular graphics representations of LOX-1 (PDB accession number: 2SBL) and mini-LOX structures were carried out through the RASMOL software (version 2.6). The hypothetical three-dimensional model of mini-LOX was derived from the LOX-1 structure following removal of the first 277 amino acids, as determined experimentally.

Analysis of Reaction Products. Both LOX-1 and mini-LOX were incubated with OD, OT, and ETE at a concentration of 40 μM in 100 mM sodium borate buffer, pH 9.0. Product formation was followed at 234 nm with a Hewlett-Packard 8452A diode array spectrophotometer, performing the reactions in a 100 mL scale. After completion, the pH was lowered to 4, and the products were extracted by solid-phase extraction (SPE) on Bakerbond (500 mg) columns (Baker, Deventer, The Netherlands). After SPE, the products were reduced with an excess of sodium borohydride at 0 °C for 30 min, and, after lowering the pH to 4, they were extracted once more by SPE and dried under a nitrogen stream. The hydroxy fatty acids were converted to the methyl esters by reaction with an excess of ethereal diazomethane for 30 min at room temperature. The products were characterized by GC/MS; for chiral separations, they were further purified by RP-HPLC. The reduced and methylated products of LOX-1 or mini-LOX reaction with different substrates were purified on a Hewlett-Packard 1090 LC HPLC system equipped with an HP 1040A diode array detector and an HP7994A analytical workstation. RP-HPLC was carried out on a Cosmosil 5C18 AR column (5 μm, 250 × 4.6 mm, Nacalai Tesque, Kyoto, Japan), using methanol/tetrahydrofuran/water/acetic acid (30:30:40:0.1, v/v/v/v) as eluent, at a flow rate of 1 mL/min. Chiral-phase HPLC separations of the reduced and methylated products were carried out on a

Chiracel OD-R column (5 μm, 250 × 4.6 mm, Daicel, Deventer, The Netherlands) with methanol/water/acetic acid as eluent, at a flow rate of 0.5 mL/min. The composition of the latter eluent was 85:15:0.1 (v/v/v) for the OD and OT products, and 80:20:0.1 (v/v/v) for the ETE products.

For the preparation of racemic 13-HOD, 13-HOT, and 15-HETE, an aliquot of the products formed by LOX-1 with OD, OT, and ETE as substrate was reduced, and then reoxidized essentially as described (*30*). Briefly, 1 μmol of hydroxy fatty acid was exposed to 6.5 mM DDQ (260 μL in diethyl ether), for 1.5 min at room temperature. The reaction was stopped by addition of 120 μL of 2-propanol and dried under a stream of nitrogen. Subsequently, methanol (1 mL) and 50 mM sodium acetate at pH 4 (10 mL) were added, and the reaction products were extracted by SPE on Bakerbond (500 mg) columns. The resulting oxo fatty acids were reduced, extracted, and methylated as described above. The racemic hydroxy fatty acid methyl esters were purified by the above RP-HPLC procedure, using methanol/water/acetic acid (80:20:0.1, v/v/v) as eluent. The reaction yields two double bond isomers, namely, the cis-trans and the trans-trans isomer, which can be easily separated because the cis-trans elutes before the trans-trans isomer.

For gas chromatography/mass spectrometry (GC/MS) analysis, the reduced methyl ester products were hydrogenated and trimethylsialylated as reported (*31*). The reduced methyl ester products were dissolved in 1 mL of hexane and hydrogenated with a catalytic amount of palladium on calcium carbonate in a hydrogen atmosphere. After 30 min, the catalyst was removed by filtration over a cotton wool prewashed with hexane. Hexane was removed under a nitrogen stream, and 100 μL of silylation reagent (pyridine/1,1,1,3,3,3-hexamethyldisilazane/trimethylchlorosilane, 5:1:1, v/v/v) was added. After 30 min at room temperature, the silylation reagent was evaporated under a gentle stream of nitrogen, and the residue was redissolved in 20 μL of hexane. An aliquot was analyzed by GC/MS, using a Carlo Erba GC 8060 with a Fisons MD 800 mass detector (Interscience, Breda, The Netherlands), equipped with a AT-1 column (30 m × 0.25 mm × 0.25 μm, Alltech, Breda, The Netherlands). The column temperature was kept for 2 min at 140 °C; then it was raised to 280 °C with 6 °C/min increments and kept at this temperature for 2 min. Mass spectra were recorded under the electron impact mode with an ionization energy of 70 eV.

Binding Experiments. Negatively charged, unsaturated phosphatidylcholine liposomes were prepared in phosphate-buffered saline according to (*32*), using the liposome kit (Sigma) as reported (*33*). The size of the vesicles was ∼2 μm, as determined under the microscope by comparison with the size (10 ± 0.5 μm) of Mono Q beads (Amersham Pharmacia Biotech, Uppsala, Sweden). The binding of LOX-1 or mini-LOX to liposomes was determined essentially as reported (*34*). Liposome suspensions corresponding to 1 μmol of phosphatidylcholine (50 μL) were incubated for 30 min at 25 °C with LOX-1 or mini-LOX (2 μM each, corresponding to 100 pmol/test), alone or in the presence of 10 μM $CaCl_2$ or 10 μM $CaCl_2$ + 100 μM EDTA. The enzyme−liposome complexes were separated by flotation on a linear sucrose density gradient (*34*); then an enzyme-linked immunosorbent assay (ELISA) was performed by coating the plate with enzyme−liposome complexes (50 μL/
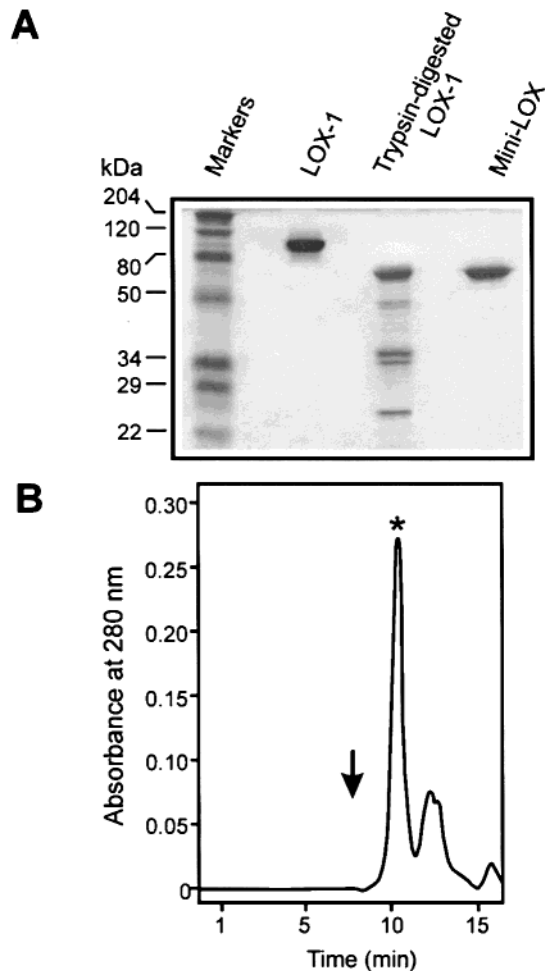
A

B

FIGURE 1: Electrophoretic and chromatographic analysis of LOX-1 and mini-LOX. (A) 12% SDS−polyacrylamide gel electrophoresis (20 μg/lane) of soybean lipoxygenase-1 (LOX-1), of its trypsin digestion products, and of the purified 60 kDa fragment (mini-LOX). Molecular mass markers are shown on the left-hand side of the gel. (B) HPLC profile of the tryptic fragments of LOX-1 (50 μg/injection) separated by gel-filtration. The arrow indicates the expected position of a 90 kDa protein, whereas the asterisk indicates the mini-LOX peak.

well). Specific anti-LOX-1 monoclonal antibodies (*35*), diluted 1:400, were used as first antibody, and goat anti-mouse alkaline phosphatase conjugate (Bio-Rad, Richmond, CA), diluted 1:2000, as second antibody (*35*). Color development of the alkaline phosphatase reaction was measured at 405 nm, using *p*-nitrophenyl phosphate as substrate. Controls were carried out by using nonimmune mouse serum (Nordic Immunology, Tilburg, The Netherlands) and included wells coated with different amounts of bovine serum albumin. The ELISA test was calibrated using different amounts of LOX-1 or mini-LOX (in the range 0−40 pmol/well), in the presence of liposomes (1 μmol of phosphatidylcholine/well).

Statistical Analysis. Data reported in this paper are the mean (±SD) of at least four independent determinations, each performed in triplicate. Statistical analysis was performed by the nonparametric Mann−Whitney test, elaborating experimental data by means of the InStat program (Graph-PAD Software for Science, San Diego, CA). Each reported electrophoretic or chromatographic profile is representative of four independent experiments.
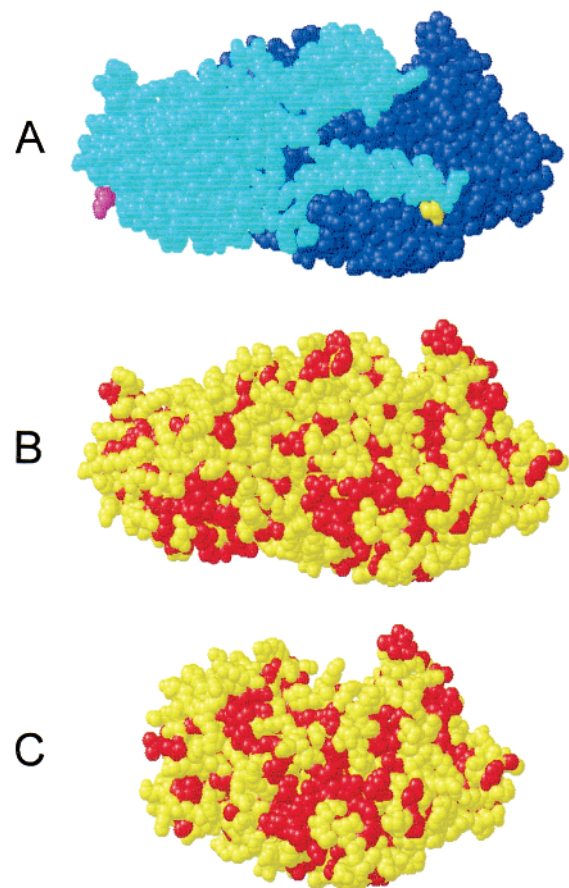

FIGURE 2: Spacefill models of LOX-1 and mini-LOX. (A) Three-dimensional structure of soybean lipoxygenase-1 (LOX-1), showing in light blue the N-terminal domain removed by trypsin digestion (∼30 kDa) and in dark blue the remaining ∼60 kDa fragment (mini-LOX). The pink residue represents the N-terminal amino acid; the yellow one represents the trypsin cleavage site generating mini-LOX (lysine 277). (B) and (C) show the spacefill models of LOX-1 and mini-LOX, respectively, in the same orientation as in (A), with hydrophobic residues in red.

RESULTS

Generation, Separation, and Characterization of Mini-LOX. Lipoxygenase-1 (LOX-1) from soybeans was digested with trypsin at a LOX-1:trypsin 10:1 (w/w) ratio, which allowed completion of the reaction within 30 min. Tryptic fragments separated by 12% SDS−polyacrylamide gel electrophoresis showed a major band of approximately 60 kDa and minor bands of lower molecular mass (Figure 1A). A similar profile was found in a previous report (*20*). The 60 kDa fragment was isolated by gel-filtration and eluted after 10 min as a single peak (Figure 1B). This fragment, referred to as "mini-LOX", was found to be electrophoretically pure on 12% SDS−polyacrylamide gels (Figure 1A). The N-terminal amino acid analysis of mini-LOX showed the sequence STPIEFHSFQ, which corresponds to a unique trypsin cleavage site between lysine 277 and serine 278 (Figure 2A). Such a cleavage should indeed remove a ∼30 kDa N-terminal domain of LOX-1, leading to a fragment of the expected molecular mass of 63 695 Da (*9, 10, 19*). These data are consistent with the electrophoretic (Figure 1A) and chromatographic (Figure 1B) properties of mini-LOX. IEF analysis on native gels (not shown) indicated that mini-LOX was slightly more acidic than LOX-1, having a p*I* of 5.6 compared to p*I* = 6.0 for the native enzyme.
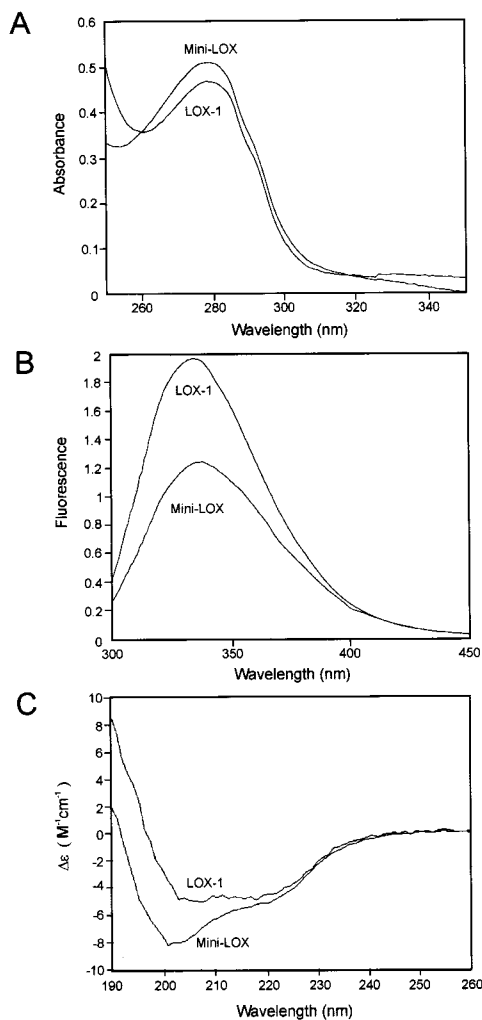
FIGURE 3: Spectroscopic properties of LOX-1 and mini-LOX. (A) Near-UV absorption spectra, (B) fluorescence emission spectra, and (C) circular dichroism spectra of soybean lipoxygenase-1 (LOX-1) and of the purified ~60 kDa fragment generated by trypsin digestion (mini-LOX). LOX-1 and mini-LOX were used at a final concentration of 10 μM (UV) or 250 nM (fluorescence and circular dichroism).

Spectroscopic Properties of LOX-1 and Mini-LOX. Native LOX-1 contains 13 tryptophan residues, 2 of which (W87 and W130) are located in the N-terminal domain. The structure of the protein at 1.4 Å resolution (*10*) has shown that most of the 13 tryptophan residues are located in hydrophobic environments. Mini-LOX showed a UV absorption spectrum substantially similar to that of LOX-1, though about 10% more intense around 280 nm (Figure 3A), but a remarkably different intrinsic fluorescence upon excitation at 284 nm (Figure 3B). Emission maxima were at 333 nm for LOX-1 and at 338 nm for mini-LOX, which is indicative of a somewhat greater exposure of aromatic chromophores to the solvent. Fluorescence emission decreased by about 40% in mini-LOX compared to LOX-1, which can be attributed not only to the loss of the two tryptophan residues present in the N-terminal domain of LOX-1 (*19*), but also to conformational changes leading to a greater solvation of some tryptophans. Accordingly, the intrinsic fluorescence of mini-LOX showed a larger full width at half-maximum, which is diagnostic of a larger heterogeneity of the protein. Also the secondary structures of LOX-1 and mini-LOX, as indicated by the far-UV CD spectrum, differed considerably
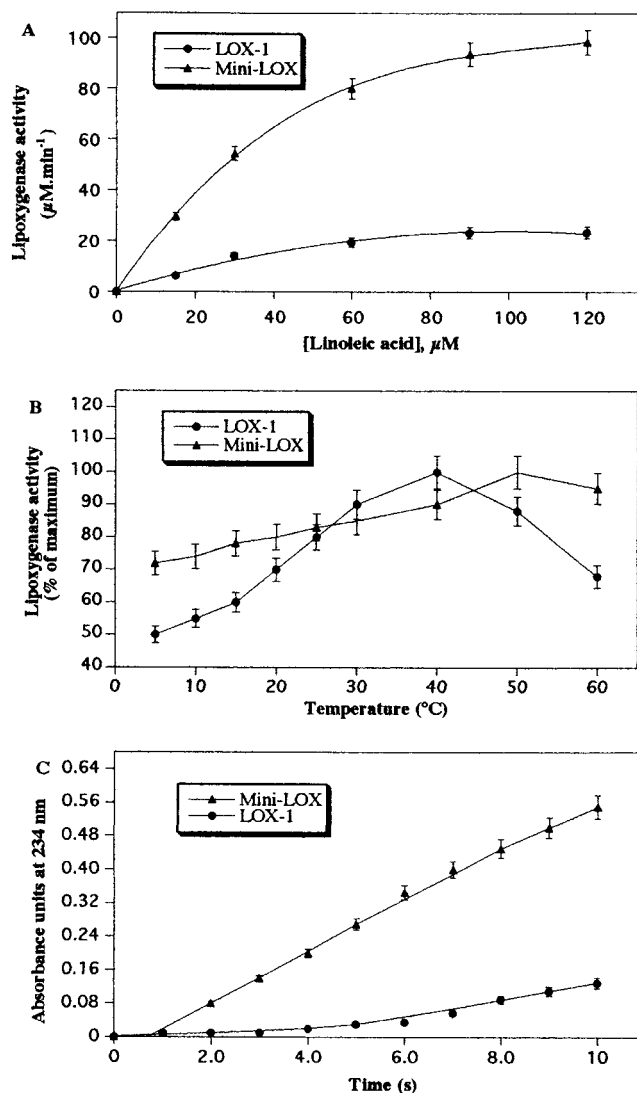

FIGURE 4: Kinetic properties of LOX-1 and mini-LOX. (A) Dependence on substrate concentration of the dioxygenation of linoleic acid by soybean lipoxygenase-1 (LOX-1) and by the purified ~60 kDa fragment generated by trypsin digestion (mini-LOX), each used at 7.5 nM, at pH 9.0 and at 25 °C. (B) Temperature dependence of the dioxygenation of 60 μM linoleic acid by 7.5 nM LOX-1 and mini-LOX, at pH 9.0. Values were expressed as percentage of the maximum (100% = 26 ± 3 and 98 ± 10 μM·min^{-1} for LOX-1 and mini-LOX, respectively). (C) Progress curves of the dioxygenation of 60 μM linoleic acid, at pH 9.0 and 25 °C, by 7.5 nM LOX-1 or mini-LOX.

(Figure 3C). Mini-LOX showed a smaller proportion of random coil and a larger proportion of α-helix (Figure 3C).

Kinetic Properties of LOX-1 and Mini-LOX. LOX-1 and mini-LOX activity depended on substrate (linoleic acid, OD) concentration according to Michaelis−Menten kinetics (Figure 4A), yielding apparent K_m values of 11.2 ± 0.6 and 24.2 ± 1.2 μM and V_{max} values of 55 ± 3 and 363 ± 18 μM·min^{-1}, respectively. From the V_{max} values, it was possible to calculate the reaction catalytic constant (k_{cat}), which was 122 and 807 s^{-1} for LOX-1 and mini-LOX, respectively. Moreover, it was possible to calculate the catalytic efficiency (expressed as k_{cat}/K_m ratio), which was 10.9 × 10^6 and 33.3 × 10^6 M^{-1}·s^{-1} for LOX-1 and mini-LOX, respectively. Table 1 summarizes the kinetic parameters of both enzyme forms. The activity of LOX-1 and mini-LOX was assayed in the pH range 3−12, and in the temperature range 5−60 °C. Both

Table 1: Kinetic Parameters of Soybean Lipoxygenase-1 (LOX-1) and of the Purified ∼60 kDa Fragment Generated by Trypsin Digestion (Mini-LOX)[a]

parameter	LOX-1	mini-LOX
K_m (μM)	11.2 ± 0.6	24.2 ± 1.2
V_{max} (μM·min^{-1})	55 ± 3	363 ± 18
k_{cat} (s^{-1})	122	807
k_{cat}/K_m (M^{-1}·s^{-1})	10.9×10^6	33.3×10^6
E_a (kJ·mol^{-1})	8.3 ± 0.9	4.5 ± 0.5
K_i for OA (μM)[b]	69 ± 7	54 ± 5

[a] The enzymatic activity of LOX-1 and mini-LOX was assayed spectrophotometrically by monitoring conjugated hydroperoxide formation from linoleic acid at 234 nm. Apparent K_m and V_{max} values were calculated by nonlinear regression analysis of the experimental data points. Catalytic constants (k_{cat}) were calculated from V_{max} values. Activation energy (E_a) was calculated by Arrhenius diagrams of the dioxygenation of linoleic acid in the temperature range 20−45 °C. [b] Oleic acid (OA) was found to act as a competitive inhibitor of both LOX-1 and mini-LOX.

enzymes showed a similar bell-shaped curve as a function of pH, with an optimum at pH = 9.5 and loss of activity at pH ≤ 4.0 (not shown). This observation corroborates and extends a recent report on LOX-1 and its 60 kDa chymotryptic fragment (*13*). The thermal stability of the two enzymes was different, LOX-1 showing a bell-shaped curve in the range 5−60 °C, with a maximum at 40 °C, whereas mini-LOX showed an almost linear increase in the same temperature range (Figure 4B). Arrhenius diagrams of OD dioxygenation in the temperature range 20−45 °C (*25*) allowed calculation of activation energies of 8.3 ± 0.9 and 4.5 ± 0.5 kJ·mol^{-1} for LOX-1 and mini-LOX, respectively (Table 1). Furthermore, oleic acid was found to be a competitive inhibitor of both LOX-1 and mini-LOX with OD as substrate, with inhibition constants of 69 ± 7 and 54 ± 5 μM (Table 1). Progress curves of the dioxygenation of 60 μM OD by 7.5 nM enzyme, at pH 9.0, showed a reaction lag phase of approximately 5 or 1 s, for LOX-1 or mini-LOX, respectively (Figure 4C). At the same pH of 9.0, LOX-1 dioxygenated 60 μM OD, α-linolenic acid (OT), arachidonic acid (ETE), or linoleate methyl ester (OD-Me) at rates of 20.2 ± 1.2, 2.4 ± 0.2, 4.2 ± 0.3, or 1.6 ± 0.2 μM·min^{-1}, respectively. With the same substrates, mini-LOX showed reaction rates of 80.8 ± 4.8, 7.2 ± 0.6, 10.5 ± 0.7, and 1.9 ± 0.2 μM·min^{-1}, respectively. Therefore, the enhanced activity of mini-LOX compared to LOX-1 was approximately 4-fold, 3-fold, 2.5-fold, and 1.2-fold, with OD, OT, ETE, or OD-Me, respectively. Remarkably, trypsin-digested LOX-1, or mini-LOX in the presence of the tryptic fragments of molecular mass <60 kDa, showed the same activity as pure mini-LOX toward the same substrates (not shown).

Analysis of LOX-1 and Mini-LOX Products. OD, OT, and ETE were incubated with LOX-1 or mini-LOX, and the reaction products were analyzed by GC/MS after reduction, methylation, hydrogenation, and trimethylsilylation. The product profiles of LOX-1 and mini-LOX were superimposable for all substrates (Figure 5A,B). The mass spectra of the reaction products are shown in Figure 5C−E. The main product of OD dioxygenation was 13-HPOD (Figure 5C), which showed diagnostic fragments at m/z 371 (M$^+$−15), 315 [TMSO$^+$=CH−(CH$_2$)$_{11}$COOCH$_3$], 173 [TMSO$^+$=CH−(CH$_2$)$_4$CH$_3$], and 73 (TMS$^+$). Also 9-HPOD (Figure 5D) could be detected, based on the characteristic fragments

at m/z 371 (M$^+$−15), 259 [TMSO$^+$=CH−(CH$_2$)$_7$COOCH$_3$], 229 [TMSO$^+$=CH−(CH$_2$)$_8$CH$_3$], and 73 (TMS$^+$). When OT was used as a substrate, the only product formed was 13-HPOT, which has the same mass spectrum as 13-HPOD (Figure 5C). Dioxygenation of ETE yielded 15-HPETE (Figure 5E) as the main product, with diagnostic fragments at m/z 399 (M$^+$−15), 343 [TMSO$^+$=CH−(CH$_2$)$_{13}$COOCH$_3$], 173 [TMSO$^+$=CH−(CH$_2$)$_4$CH$_3$], and 73 (TMS$^+$). If the enzymatic reaction was allowed to proceed for longer times and at higher enzyme concentrations, also 8,15- and 5,15-diHPETE were detected, upon reaction with either LOX-1 or mini-LOX (not shown). The chiral analysis of the main reaction products obtained after incubation of OD, OT, and ETE with LOX-1 and mini-LOX is shown in Figure 6. Both lipoxygenases showed a strict enantiomeric purity of the main products, whatever the substrate used. To further corroborate this finding, the products were co-injected with their racemic counterparts, which showed that the second peak (the *S* enantiomer) arose in all cases (data not shown). Since LOX-1 is known to always produce the *S* enantiomer, these results demonstrate that also mini-LOX does produce only the *S* enantiomer with all the substrates tested.

Binding of LOX-1 and Mini-LOX to Membranes. Anti-LOX-1 monoclonal antibody (*35*) was able to recognize in the same way both LOX-1 and mini-LOX in the presence of negatively charged, unsaturated liposomes (Figure 7A). This antibody was used to quantify by ELISA the amount of LOX-1 or mini-LOX bound to these vesicles. It was found that both enzymes were able to bind to liposomes, mini-LOX showing a 60% higher binding ability than LOX-1 (Figure 7B). In the presence of calcium ions, the amount of LOX-1 bound to membranes increased 3.5-fold, whereas mini-LOX increased only 2-fold, compared to the corresponding controls without calcium (Figure 7B). The calcium chelator EDTA fully reverted the effect of calcium on the binding of each enzyme to the membranes (Figure 7B). In this context, it seems noteworthy that RP-HPLC analysis of trypsin-digested LOX-1 showed the main peak (mini-LOX) eluting after 27 min, whereas LOX-1 eluted after 24 min under the same conditions. This indicates that mini-LOX is more hydrophobic than LOX-1, in keeping with the three-dimensional models showing that hydrophobic residues shielded in LOX-1 by the N-terminal domain are exposed to the solvent in mini-LOX (Figure 2B,C).

DISCUSSION

Limited proteolysis by trypsin (*12, 20*) or by chymotrypsin (*13, 20, 21*) has shown that two major fragments can be obtained from LOX-1: an N-terminal domain of ∼30 kDa and a C-terminal domain of ∼60 kDa. In this study, the ∼60 kDa tryptic fragment, referred to as "mini-LOX", was purified without denaturation steps (Figure 1B), and was shown to originate from the cleavage between lysine 277 and serine 278 (Figure 2A). Since the further potential 53 trypsin cleavage sites in the 60 kDa C-terminal domain were not cleaved, it can be speculated that these residues are not freely accessible. Interestingly, the determined p*I* values of LOX-1 (6.0) and mini-LOX (5.6) were in keeping with those calculated, i.e., 5.96 and 5.74, respectively. Moreover, the spectroscopic analysis of LOX-1 and mini-LOX, showing an increased α-helix content in the latter compared to the former enzyme (Figure 3C), is consistent with secondary
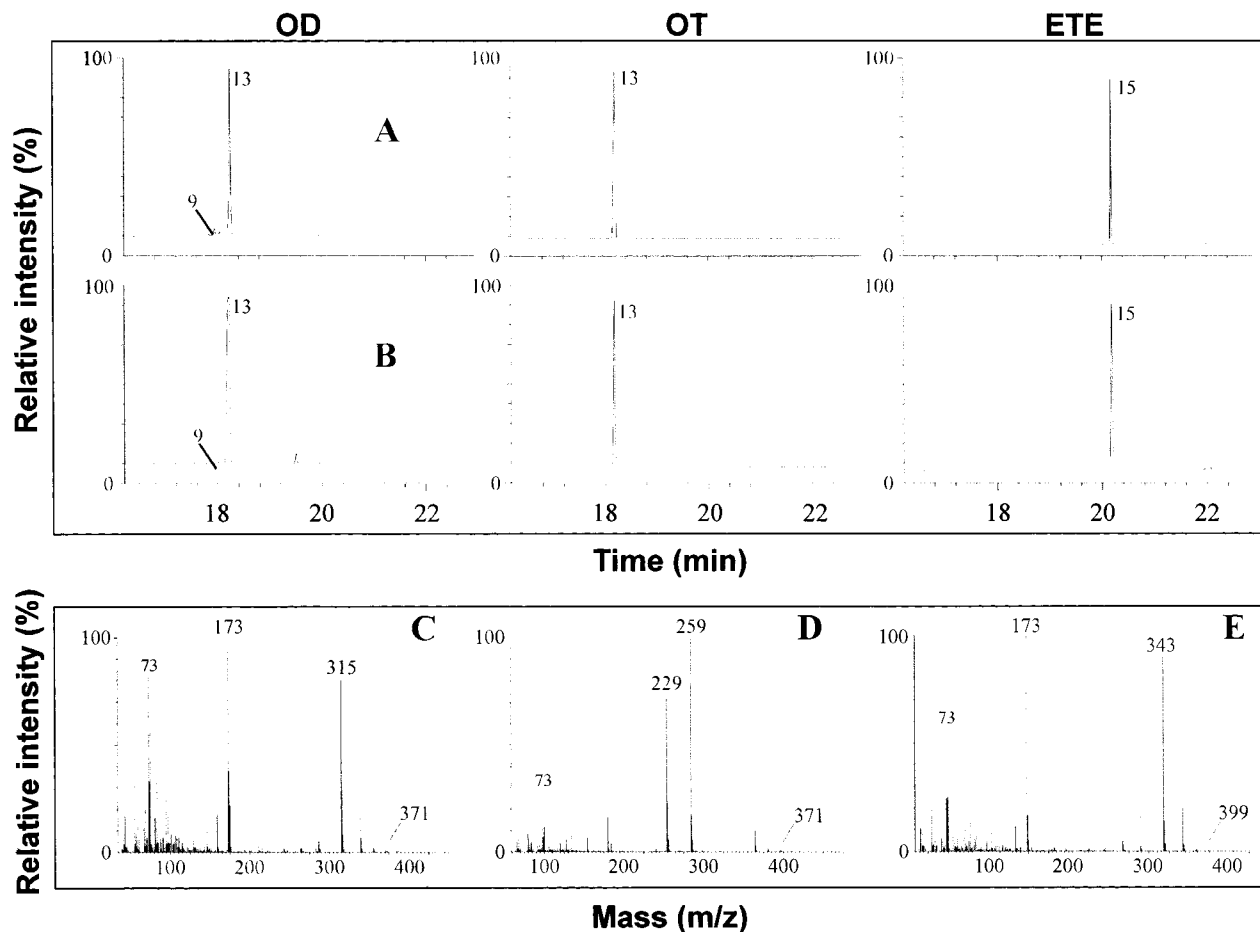
FIGURE 5: GC/MS analysis of the products of LOX-1 and mini-LOX. Linoleic acid (OD), α-linolenic acid (OT), and arachidonic acid (ETE) were incubated with soybean lipoxygenase-1 (LOX-1) or with the purified ∼60 kDa fragment generated by trypsin digestion (mini-LOX). The reaction products of LOX-1 (A) and mini-LOX (B) were analyzed by GC/MS. Mass spectra of the products of LOX-1 and mini-LOX derived from incubations of OD (C and D), OT (C), and ETE (E) after reduction, methylation, hydrogenation, and trimethylsilylation. (C) = 13-HPOD, 13-HPOT; (D) = 9-HPOD; (E) = 15-HPETE.
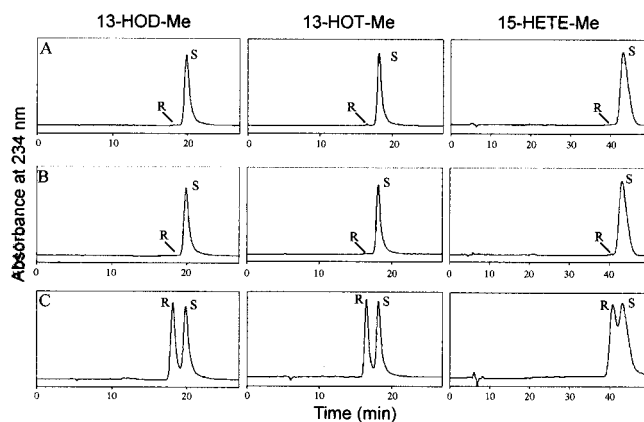

FIGURE 6: Chiral-phase HPLC of the products of LOX-1 and mini-LOX. Main products formed upon incubation of linoleic acid (13-HOD-Me), α-linolenic acid (13-HOT-Me), or arachidonic acid (15-HETE-Me) with soybean lipoxygenase-1 (LOX-1, panel A) or with the purified ∼60 kDa fragment generated by trypsin digestion (mini-LOX, panel B). (C) Racemic products of linoleic, α-linolenic, or arachidonic acids, synthesized as described under Experimental Procedures.

structure calculations through singular value decomposition fitting (*36*), which indicate that LOX-1 contains 35.6% α-helix, whereas mini-LOX contains 46.6%. These data extend a previous report, showing that the 60 kDa chymo-tryptic fragment of LOX-1 has more α-helix than the native LOX-1 (*21*).

A major finding of this investigation is that mini-LOX is an active enzyme, which has an even greater catalytic efficiency compared to native LOX-1 (Figure 4A and Table 1). Mini-LOX showed approximately 2-fold higher K_m and 7-fold higher V_{max} (and k_{cat}) values compared to LOX-1, leading to a 3-fold higher catalytic efficiency (Table 1). Consistently, the activation energy (E_a) of the reaction catalyzed by LOX-1, close to that reported elsewhere (*37*), was 2-fold higher than that of the reaction catalyzed by mini-LOX (Table 1). To better understand the mechanism of the enhanced activity of mini-LOX, progress curves of the enzymatic reaction were recorded. Lipoxygenase-catalyzed dioxygenation shows an initial "kinetic lag phase" or "induction period", which is needed to convert the inactive iron(II) into the active iron(III) enzyme by the contaminant hydroperoxides normally present in substrate preparations (*38*). The initial reaction rate of lipoxygenase catalysis is inversely proportional to the duration of the lag phase (*14*). In our experimental conditions, the dioxygenation of OD by LOX-1 showed a lag phase of ∼5 s, in line with previous stopped-flow measurements (*38*), while the lag phase of mini-LOX was shortened to ∼1 s (Figure 4C). This finding may suggest that removal of the N-terminal domain facilitates the oxidation of iron(II) to iron(III). However, EPR spec-
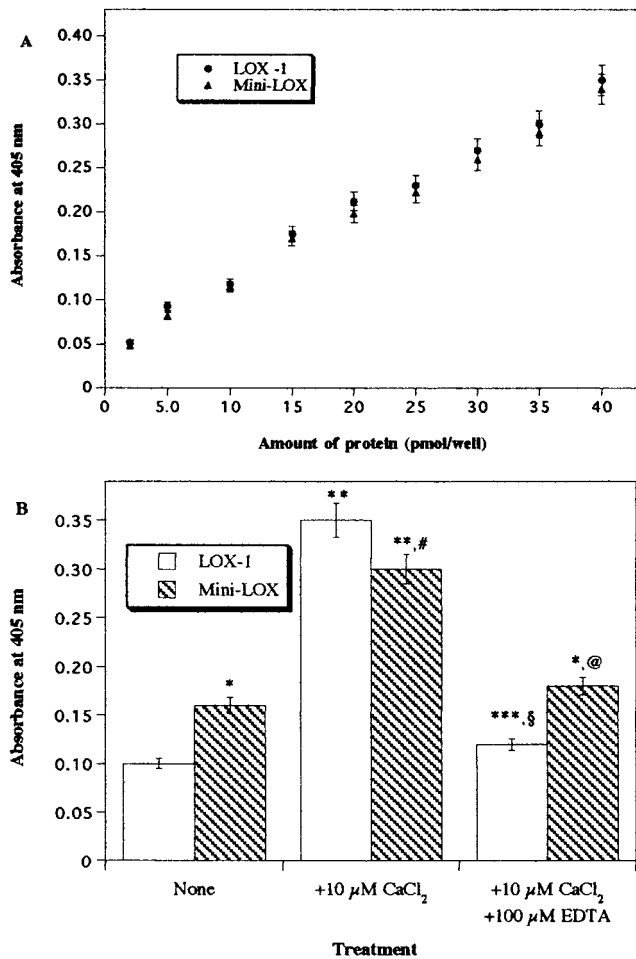
FIGURE 7: Binding of LOX-1 and mini-LOX to membranes. (A) Calibration of the enzyme-linked immunosorbent assay (ELISA) for soybean lipoxygenase-1 (LOX-1) and the purified ∼60 kDa fragment generated by trypsin digestion (mini-LOX), in the presence of negatively charged, unsaturated liposomes (1 μmol of phosphatidylcholine/well). (B) Quantitation by ELISA of the amount of LOX-1 or mini-LOX bound to liposomes, in the presence or absence of 10 μM CaCl$_2$ or 10 μM CaCl$_2$ + 100 μM EDTA. (*) denotes $p < 0.05$ compared to LOX-1 (none); (**) denotes $p < 0.01$ compared to LOX-1 (none); (***) denotes $p > 0.05$ compared to LOX-1 (none); (#) denotes $p < 0.01$ compared to mini-LOX (none); (§) denotes $p < 0.01$ compared to LOX-1 (+CaCl$_2$); (@) denotes $p < 0.01$ compared to mini-LOX (+CaCl$_2$).

troscopy has shown that the iron environment is the same in native and trypsin-digested LOX-1 (*20*); therefore, alternatively it can be proposed that enhanced mini-LOX activity is due to a more productive binding of the substrate to the enzyme or to a faster dissociation of the product. In any case, LOX-1 and mini-LOX showed the same substrate preference, in the order OD ≫ ETE > OT, though the difference in activity between the two enzymes decreased from OD, to OT or ETE. Both LOX-1 and mini-LOX hardly acted on esterified substrates such as OD-Me (Figure 4C), confirming that a free carboxylic group in the substrate is needed to bind positively charged amino acids in the active site of the enzyme (*11*). Most notably, both enzymes showed identical product profiles, with respect to regio- and stereospecificity (Figures 5 and 6). Taken together, these findings provide substantial evidence that the active site conformation of LOX-1 is retained in mini-LOX. The inhibition by oleic acid, showing similar K_i values for both enzymes (Table 1), further strengthens this hypothesis. In this context, it seems also

noteworthy that trypsin-digested LOX-1, as well as "reconstituted" LOX-1 obtained by adding to mini-LOX the tryptic fragments of molecular mass <60 kDa, showed the same activity as pure mini-LOX, suggesting that these <60 kDa fragments had no effect on enzyme activity. This result is at variance with a previous report showing that the <60 kDa fragments were necessary for the activity of digested LOX-1 (*20*). On the other hand, an inhibition of mini-LOX by these fragments could be expected, based on the enhanced activity of the trimmed enzyme compared to the native form. It can be proposed that the lack of effect (either stimulatory or inhibitory) of the <60 kDa fragments on mini-LOX activity simply reflects a different interaction between the N-terminal and C-terminal fragments upon proteolysis.

An important issue regarding lipoxygenases is their ability to bind and modify biomembranes, as reported for both animals (*39*) and plants (*40*). Indeed, LOX-1 has been shown to utilize phospholipids in lipid bilayers (*41*), and fatty acids inserted into phospholipid micelles (*16*), as physiological substrates. Such activity has received increasing interest since the discovery that lipoxygenase forms pore-like structures in biomembranes, thus leading to programmed organelle degradation (*42*). Nevertheless, it is still unclear how this membrane binding is regulated, though recent evidence strongly suggests that soybean LOX-1 (*43*) and also human 5-lipoxygenase (*44*) and 15-lipoxygenase (*45*) bind membranes through a calcium-dependent mechanism. Here we show that mini-LOX binds artificial membranes better than does LOX-1 (Figure 7B), in keeping with the higher hydrophobicity of the former enzyme observed by RP-HPLC and with the three-dimensional model. This model (Figure 2) shows that the inner core of LOX-1 is shielded by the N-terminal domain in the native enzyme but exposed to the solvent in the mini-LOX, and is highly hydrophobic (Figure 2C). Remarkably, calcium enhanced LOX-1 affinity for membranes by approximately 4-fold, while it enhanced mini-LOX affinity by approximately 2-fold only (Figure 7B). This finding might be explained by the presence of two calcium binding sites in LOX-1, one in the N-terminal domain and the other one in the C-terminal domain, as suggested by previous spectroscopic evidence (*43*). However, the different effect of calcium on (mini-)LOX binding properties might also reflect the enhanced ability of mini-LOX to bind to these vesicles in the absence of calcium (presumably due to its enhanced hydrophobicity). At any rate, the observation that the N-terminal domain affects the binding of LOX-1 to membranes extends to this enzyme recent observations on lipid body lipoxygenase (*34*) and human 5-lipoxygenase (*46*).

In conclusion, it is tempting to suggest that the 30 kDa fragment is a built-in inhibitor of soybean LOX-1, in analogy to external modulators of enzyme activity such as the 5-lipoxygenase activating protein (*47*). Removal of this built-in inactivator by intracellular proteases generates a lipoxygenase with improved activity and membrane binding ability. The trimmed enzyme might play a role in physio(patho)-logical conditions, where enhanced lipoxygenase activity and membrane lipoperoxidation have been observed, such as kidney disease in humans (*5*) and programmed cell death in plants (*8*). In this context, it seems noteworthy that a trypsin-like protease, termed SNP1, has been shown to be produced during plant infection by pathogens (*48*), a typical situation where lipoxygenase is known to be activated (*49, 50*).

REFERENCES

1. Kühn, H., and Borngraber, S. (1999) *Adv. Exp. Med. Biol. 447*, 5−28.
2. Cathcart, M. K., and Folcik, V. A. (2000) *Free Radical Biol. Med. 28*, 1726−1734.
3. Manev, H., Uz, T., Sugaya, K., and Qu, T. (2000) *FASEB J. 14*, 1464−1469.
4. Maccarrone, M., Bari, M., Corasaniti, M. T., Nisticò, R., Bagetta, G., and Finazzi-Agrò, A. (2000) *J. Neurochem. 75*, 196−203.
5. Maccarrone, M., Taccone-Gallucci, M., Meloni, C., Cococcetta, N., Manca di Villahermosa, S., Casciani, U., and Finazzi-Agrò, A. (1999) *J. Am. Soc. Nephrol. 10*, 1991−1996.
6. Montero, A., and Badr, K. F. (2000) *Exp. Nephrol. 8*, 14−19.
7. Grechkin, A. (1998) *Prog. Lipid Res. 37*, 317−352.
8. Maccarrone, M., Van Zadelhoff, G., Veldink, G. A., Vliegenthart, J. F. G., and Finazzi-Agrò, A. (2000) *Eur. J. Biochem. 267*, 5078−5084.
9. Boyington, J. C., Gaffney, B. J., and Amzel, L. M. (1993) *Science 260*, 1482−1486.
10. Minor, W., Steczko, J., Stec, B., Otwinowski, Z., Bolin, J. T., Walter, R., and Axelrod, B. (1996) *Biochemistry 35*, 10687−10701.
11. Gan, Q.-F., Browner, M. F., Sloane, D. L., and Sigal, E. (1996) *J. Biol. Chem. 271*, 25412−25418.
12. Sudharshan, E., and Appu Rao, A. G. (1999) *J. Biol. Chem. 274*, 35351−35358.
13. Sudharshan, E., Srinivasulu, S., and Appu Rao, A. G. (2000) *Biochim. Biophys. Acta 1480*, 13−22.
14. Schilstra, M. J., Veldink, G. A., and Vliegenthart, J. F. G. (1994) *Biochemistry 33*, 3974−3979.
15. Glickman, M. H., and Klinman, J. P. (1996) *Biochemistry 35*, 12882−12892.
16. Began, G., Sudharshan, E., and Appu Rao, A. G. (1999) *Biochemistry 38*, 13920−13927.
17. Rickert, K. W., and Klinman, J. P. (1999) *Biochemistry 38*, 12218−12228.
18. Clapp, C. H., McKown, J., Xu, H., Grandizio, A. M., Yang, G., and Fayer, J. (2000) *Biochemistry 39*, 2603−2611.
19. Shibata, D., Steczko, J., Dixon, J. E., Hermodson, M., Yazdanparast, R., and Axelrod, B. (1987) *J. Biol. Chem. 262*, 10080−10085.
20. Ramachandran, S., Carroll, R. T., Dunham, W. R., and Funk, M. O. (1992) *Biochemistry 31*, 7700−7706.
21. Sudharshan, E., and Appu Rao, A. G. (1997) *FEBS Lett. 406*, 184−188.
22. Brash, A. R. (19997 *J. Biol. Chem. 274*, 23679−23682.
23. Finazzi-Agrò, A., Avigliano, L., Veldink, G. A., Vliegenthart, J. F. G., and Boldingh, J. (1973) *Biochim. Biophys. Acta 326*, 462−470.
24. Bradford, M. M. (1976) *Anal. Biochem. 72*, 248−254.
25. Maccarrone, M., van der Stelt, M., Rossi, A., Veldink, G. A., Vliegenthart, J. F. G., and Finazzi-Agrò, A. (1998) *J. Biol. Chem. 273*, 32332−32339.
26. Segel, I. H. (1976) *Biochemical Calculations*, pp 277−281, John Wiley & Sons, New York.
27. Robertson, E. F., Dannelly, H. K., Malloy, P. J., and Reeves, H. C. (1987) *Anal. Biochem. 167*, 290−294.
28. Compton, L. A., and Curtis Johnson, W. (1986) *Anal. Biochem. 155*, 155−167.
29. Amiconi, G., Amoresano, A., Boumis, G., Brancaccio, A., De Cristofaro, R., De Pascalis, A., Di Girolamo, S., Maras, B., and Scaloni, A. (2000) *Biochemistry 39*, 10294−10308.
30. O'Flaherty, J. T., Cordes, J. F., Lee, S. L., Samuel, M., and Thomas, M. J. (1994) *Biochim. Biophys. Acta 1201*, 505−515.
31. Van Zadelhoff, G., Veldink, G. A., and Vliegenthart, J. F. G. (1998) *Biochem. Biophys. Res. Commun. 248*, 33−38.
32. Nagao, A., and Terao, J. (1990) *Biochem. Biophys. Res. Commun. 172*, 385−389.
33. Maccarrone, M., Fantini, C., Finazzi-Agrò, A., and Rosato, N. (1998) *Biochim. Biophys. Acta 1414*, 43−50.
34. May, C., Höhne, M., Gnau, P., Schwennesen, K., and Kindl, H. (2000) *Eur. J. Biochem. 267*, 1100−1109.
35. Maccarrone, M., Veldink, G. A., and Vliegenthart, J. F. G. (1992) *Eur. J. Biochem. 205*, 995−1001.
36. Curtis Johnson, W. (1999) *Proteins: Struct., Funct., Genet. 35*, 307−312.
37. Jonsson, T., Glickman, M. H., Sun, S., and Klinman, J. P. (1996) *J. Am. Chem. Soc. 118*, 10319−10320.
38. Schilstra, M. J., Veldink, G. A., and Vliegenthart, J. F. G. (1993) *Biochemistry 32*, 7686−7691.
39. Schnurr, K., Hellwing, M., Seidemann, B., Jungblut, P., Kühn, H., Rapoport, S. M., and Schewe, T. (1996) *Free Radical Biol. Med. 20*, 11−21.
40. Feussner, I., Wasternack, C., Kindl, H., and Kühn, H. (1995) *Proc. Natl. Acad. Sci. U.S.A. 92*, 11849−11853.
41. Pérez-Gilabert, M., Veldink, G. A., and Vliegenthart, J. F. G. (1998) *Arch. Biochem. Biophys. 354*, 18−23.
42. Van Leyen, K., Duvoisin, R. M., Engelhardt, H., and Wiedmann, M. (1998) *Nature 395*, 392−395.
43. Tatulian, S. A., Steczko, J., and Minor, W. (1998) *Biochemistry 37*, 15481−15490.
44. Hammarberg, T., and Rådmark, O. (1999) *Biochemistry 38*, 4441−4447.
45. Kilty, I., Logan, A., and Vickers, P. J. (1999) *Eur. J. Biochem. 266*, 83−93.
46. Hammarberg, T., Provost, P., Persson, B., and Rådmark, O. (2000) *J. Biol. Chem. 275*, 38787−38793.
47. Bannenberg, G., Dahlen, S. E., Luijerink, M., Lundqvist, G., and Morgenstern, R. (1999) *J. Biol. Chem. 274*, 1994−1999.
48. Carlile, A. J., Bindschedler, L. V., Bailey, A. M., Bowyer, P., Clarkson, J. M., and Cooper, R. M. (2000) *Mol. Plant-Microbe Interact. 13*, 538−550.
49. Buonaurio, R., and Servili, M. (1999) *Physiol. Mol. Plant Pathol. 54*, 155−169.
50. Rusterucci, C., Montillet, J. L., Agnel, J. P., Battesti, C., Alonso, B., Knoll, A., Bessoule, J. J., Etienne, P., Suty, L., Blein, J. P., and Triantaphylides, C. (1999) *J. Biol. Chem. 274*, 36446−36455.